Self-Propagating Solid-Solid Noncatalytic Reactions in Finite Pellets

The method of self-propagating high-temperature synthesis (SHS) can be utilized to synthesize certain advanced ceramic materials, such as metal carbides, borides and silicides, directly from the elements in powder form. The method involves mixing the powders, preparing pellets from the mixture, and igniting one end of the pellet. Owing to high exothermicity of the reactions, a combustion wave can propagate through the pellet. The influence of processing conditions on propagation of the combustion wave is investigated extensively in this modeling study for pellets of finite length. It is shown that unlike infinitely long systems, the combustion wave for a finite pellet does not propagate in constant pattern. It is also shown that radiative heat losses play a major role in SHS, while convective heat losses are not relatively important.

Arvind Varma
Giacomo Cao
Massimo Morbidelli
Department of Chemical Engineering
University of Notre Dame
Notre Dame, IN 46556

Introduction

A novel and simple method for making certain advanced ceramic materials is the *self-propagating high-temperature synthesis* (SHS). This method was invented in the early 1970s in the Soviet Union by A. G. Merzhanov and his associates (e.g., Merzhanov and Borovinskaya, 1972). The basic concept is that once initiated, a highly exothermic reaction can become self-sustaining and will propagate through the reactant mixture in the form of a combustion wave. The reactants are converted to the product as the combustion wave advances, as shown schematically in Figure 1. Depending on the nature of the components and the experimental conditions, the combustion wave velocity can vary from 0.1–25 cm/s. The temperature in the zone of synthesis can be *very* high; for example, the adiabatic temperature rise (ΔT_{ad}) for titanium boride is 2,900°C, while for silicon nitride it is about 4,000°C. It has been suggested empirically that combustion reactions become self-sustaining for $\Delta T_{ad} \gtrsim$ 1,500°C (Munir, 1988).

The SHS method offers several advantages over conventional processes. It is a relatively simple process and does not require high-temperature furnaces or complex processing equipment. Since initiation of the reaction requires ignition of only a small area (at most one end) of the specimen, the energy requirement is relatively small. Also, owing to high temperature in the synthesis zone, impurities present in the initial reactant powders are volatilized, thus giving higher product purity. Since its initial discovery, many ceramic materials have been synthesized by this method, primarily in the Soviet Union, where the method has been developed extensively. These materials include metal borides, carbides, nitrides, and silicides. A review of the method and its current status have recently been provided by Munir (1988).

There is extensive literature, both theoretical and experimental, treating the propagation of reaction fronts in combustion systems (cf. Puszynski et al., 1987; Merzhanov and Khaikin, 1988 for recent surveys). For the propagation of combustion waves in solid reactants, however, we are not aware of any theoretical analyses dealing with specimens of finite length. Previous studies have invariably treated infinitely long systems. In the present paper, we investigate the influence of pellet length and processing conditions on the propagation of combustion waves—especially as relevant to the SHS method.

Basic Equations

In this section, we develop the heat and mass balance equations for an exothermic noncatalytic reaction, occurring between two solid materials:

$$S(s) + M(s) \rightarrow P(s). \tag{1}$$

The following assumptions are made to develop the model.

- The mixture of solid powders behaves like an isotropic mixture.

Correspondence concerning this paper should be addressed to A. Varma.
Present address of G. Cao and M. Morbidelli: Dipartimento di Ingegneria Chimica e Materiali, Universita di Cagliari, Piazza d'Armi, 09123 Cagliari, Italy.

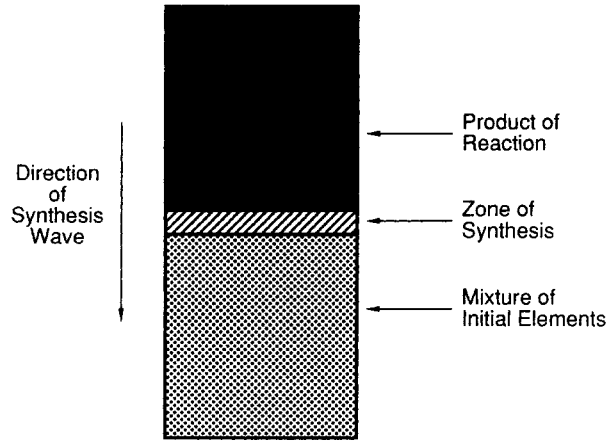

Schematic Diagram of SHS Process

Figure 1. The SHS process.

- Mass diffusion of the solid reactants and product does not occur.
- All physical properties remain constant.
- The reaction does not cause melting.
- The reaction is first-order with respect to one reactant (S), and zero-order with respect to the second reactant (M) which is present in excess.

For a cylindrical pellet of finite length, the mass and heat balances are given by

$$C_p\rho\frac{\partial T}{\partial t} = \lambda\frac{\partial^2 T}{\partial z^2} + (-\Delta H)r(C_s, T) - \frac{4U}{d}(T - T_o) - \frac{4\sigma F}{d}(T^4 - T_o^4) \quad (2)$$

$$\frac{\partial C_s}{\partial t} = -r(C_s, T) \quad (3)$$

where

$$r(C_s, T) = k_o C_s \exp(-E/RT). \quad (4)$$

The energy balance includes cooling from the external surface of the pellet, by both Newtonian and radiative mechanisms. The initial conditions (ICs) and the boundary condition (BC) at the cold end of the pellet ($z = l$) are given as

$$T = T_o, C_s = C_{so}; t = 0, 0 < z < l \quad (5)$$

$$-\lambda\frac{\partial T}{\partial z} = U(T - T_o) + \sigma F(T^4 - T_o^4); t > 0, z = l \quad (6)$$

The BC at the hot surface of the pellet ($z = 0$) depends upon the ignition procedure which is selected. Thus to initiate the process, either the $z = 0$ end is elevated to and maintained at a constant temperature, or a constant heat flux can be applied for a short period of time. These alternatives lead to the BC

$$T = T_h; t > 0, \quad z = 0 \quad (7)$$

or

$$-\lambda\frac{\partial T}{\partial z} = q; 0 < t < t_q, \quad z = 0 \quad (8a)$$

$$\lambda\frac{\partial T}{\partial z} = U(T - T_o) + \sigma F(T^4 - T_o^4); t > t_q, \quad z = 0 \quad (8b)$$

Introducing the dimensionless quantities

$$\theta = \frac{T}{T^*}, \eta = 1 - \frac{C_s}{C_{so}}, \tau = \frac{t}{t^*}, x = \frac{z}{z^*}$$

$$t^* = \frac{\exp(\gamma)}{k_o}, z^* = \left(\frac{\lambda t^*}{C_p\rho}\right)^{1/2}, L = \frac{l}{z^*}$$

$$\beta = \frac{(-\Delta H)C_{so}}{C_p\rho T^*}, \gamma = \frac{E}{RT^*}, \phi = \frac{qz^*}{\lambda T^*}$$

$$\alpha = \frac{4Ut^*}{C_p\rho d}, \psi = \frac{4\sigma F t^* T^{*3}}{C_p\rho d}, Bi = \frac{Uz^*}{\lambda},$$

$$\Omega = \frac{\sigma F z^* T^{*3}}{\lambda} \quad (9)$$

Equations 2–8 take the dimensionless form

$$\frac{\partial\theta}{\partial\tau} = \frac{\partial^2\theta}{\partial x^2} + \beta(1 - \eta)\exp\left[\gamma\left(1 - \frac{1}{\theta}\right)\right] - \alpha(\theta - \theta_o) - \psi(\theta^4 - \theta_o^4) \quad (10)$$

$$\frac{\partial\eta}{\partial\tau} = (1 - \eta)\exp\left[\gamma\left(1 - \frac{1}{\theta}\right)\right] \quad (11)$$

$$\theta = \theta_o, \eta = 0; \tau = 0, 0 < x < L \quad (12)$$

$$\theta = \theta_h; \tau > 0, x = 0 \quad (13)$$

or

$$-\frac{\partial\theta}{\partial x} = \phi; 0 < \tau < \tau_\phi, x = 0 \quad (14a)$$

$$\frac{\partial\theta}{\partial x} = Bi(\theta - \theta_o) + \Omega(\theta^4 - \theta_o^4); \tau > \tau_\phi, x = 0 \quad (14b)$$

$$-\frac{\partial\theta}{\partial x} = Bi(\theta - \theta_o) + \Omega(\theta^4 - \theta_o^4); \tau > 0, x = L \quad (15)$$

The dimensionless variables depend upon the value of the reference temperature, T^*; a convenient choice for this is the adiabatic temperature.

The Numerical Method

The governing balance equations are in the form of a nonlinear partial differential Eq. 10, coupled with an ordinary differential Eq. 11. Due to high values of both heat of reaction (β) and activation energy (γ) parameters, the reaction front is relatively sharp and its position changes with time. The temperature and concentration gradients are, therefore, steep and pose a difficult numerical problem.

In the present work, a central finite-difference scheme was adopted for the spatial derivatives in order to obtain a set of ordinary differential equations at the internal node points, which were solved as an initial value problem using the Gear method (1971).

When radiative cooling is accounted for, in both Eq. 10 and in the BC given by Eq. 15, the approximation of Eq. 10 at the last interior finite-difference point (N) gives an equation which involves θ_{N-1}, θ_N and θ_{N+1}. The latter two variables are also related nonlinearly by the BC given by Eq. 15. While computing values at the current time step, it was most efficient to fix θ_{N+1} in Eq. 10 at its value at the previous time step, thus uncoupling the equation from the boundary condition. After the finite-difference equations were solved by the Gear's method for the current time step, the value of θ_{N+1} was updated, by solving the central finite-difference analog of Eq. 15:

$$\frac{(\theta_{N+1} - 4\theta_N + 3\theta_{N-1})}{2\Delta x} = Bi(\theta_{N+1} - \theta_o) + \Omega(\theta_{N+1}^4 - \theta_o^4) \quad (16)$$

by Newton-Raphson method to give θ_{N+1}.

During the computations, the value of N was generally kept as 50, while the tolerance parameter in Gear's method was maintained as 10^{-7}. Higher values of N and lower values of the tolerance parameter did not cause any perceptible change in the results.

Results and Discussion

As noted in the Introduction section, we have two primary aims for the present investigation: i) influence of finite pellet length, and ii) influence of process operating conditions.

The range of the dimensionless parameters used for the computations are typical of SHS process, as given in Table 1. The kinetic parameters were taken from the values reported in the literature (Borovinskaya et al., 1974; Puszynski et al., 1987; Kumar et al., 1988) and are representative of reaction systems such as Mo + Si, Ti + B, Ti + C, and Zr + B. The characteristic time for chemical reaction, t^* ranges from 10^{-3} to 1 s, and consequently the characteristic length, z^* over which conduction occurs effectively during time t^* ranges from 0.15 to 5 mm. The values of heat transfer coefficients required for the convective heat loss parameters, α and Bi were calculated for natural convection (cf. Bird et al., 1960) under typical SHS conditions. Similarly, the range for the radiative heat loss parameters ψ and Ω was also estimated for typical SHS conditions.

Adiabatic case

The adiabatic case was investigated first. In this case, heat transfer from the surface and the ends, by both convection and radiation, is neglected ($\alpha = \psi = Bi = \Omega = 0$). Figure 2 corresponds to the case where the $x = 0$ end is suddenly elevated to

Table 1. Values of Dimensionless Parameters in Typical SHS Processes

β	0.5–1	α	0–0.02
γ	10	Ψ	0–1
L	0–10	Bi	0–0.03
ϕ	0–30	Ω	0–1

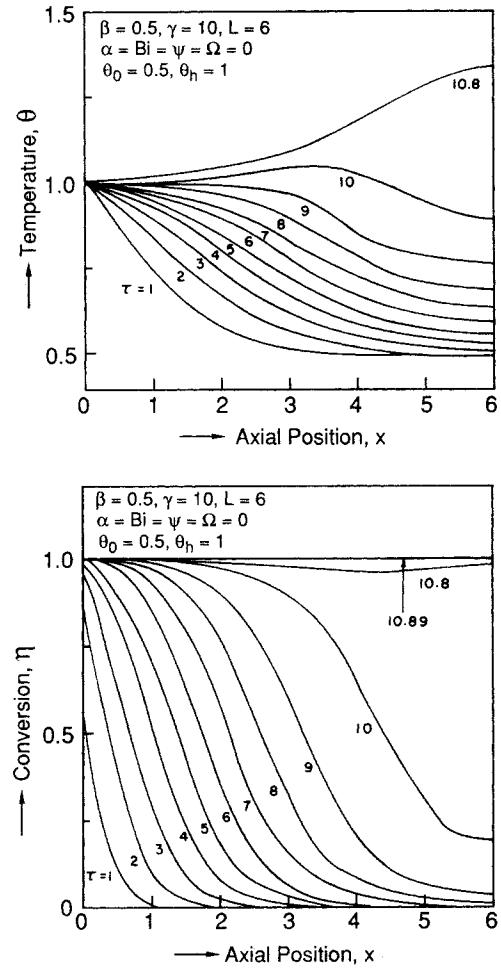

Figure 2. Time-space temperature and conversion profiles, in which one end of the pellet is maintained at a fixed temperature, boundary condition of Eq. 13.

and maintained at temperature θ_h, the BC of Eq. 13. The propagation of the reaction wave for both temperature and conversion can be seen readily. The pellet is completely reacted at a value of τ equal to about 10, which for $t^* = 1$ s would correspond to a process time of ~10 s. It is quite clear from the temperature profiles in Figure 2a that the pellet initially receives heat from the $x = 0$ end and later loses heat through this same end in order to maintain the BC at $x = 0$. In this sense, the system is in fact nonadiabatic; the term *adiabatic* is used only to stress that heat losses are not explicitly accounted for in the model.

Figure 3 corresponds to the BC of Eq. 14; thus a heat flux ϕ is applied at the $x = 0$ end for only a short duration τ_ϕ. In this case, depending on the value of ϕ, the temperature near $x = 0$ can attain relatively high values, and for this reason the pellet reacts completely when τ reaches about 4.5.

Figures 2a and 3a show that when the synthesis is initiated, the maximum temperature in the system occurs at $x = 0$. This point remains the hottest point of the system for about two-thirds of the pellet reaction time, when the location of the maximum temperature moves suddenly to a position somewhere well inside the pellet ($x \simeq 2.5$), and then it moves quickly toward

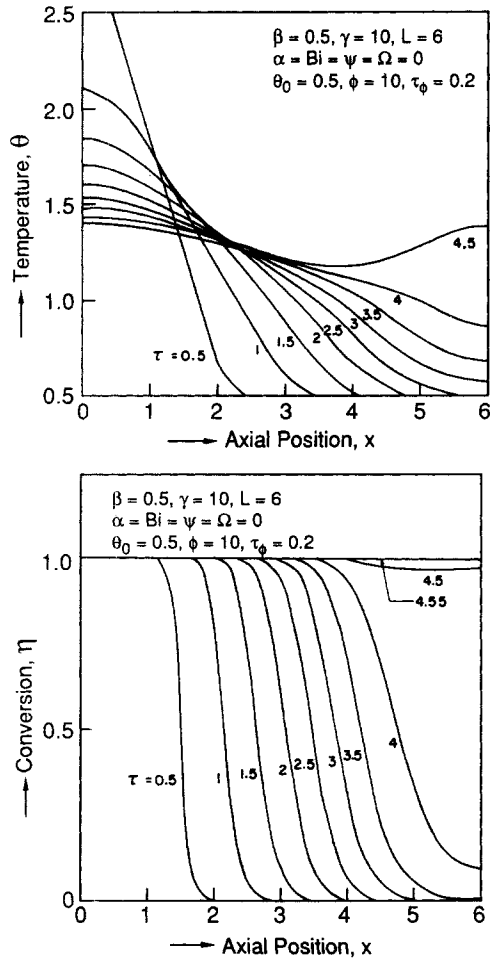

Figure 3. Time-space temperature and conversion profiles with specified heat flux at one end of the pellet, boundary condition of Eq. 14.

the $x = L$ end of the pellet. During this period, the reaction front moves rather rapidly because the entire pellet has by now been brought to a relatively high temperature by heat conduction. The reaction therefore occurs fast, fully converting the remainder of the pellet. For this reason, temperature near the $x = L$ end increases sharply to relatively high values. Subsequently, the pellet simply cools by heat transfer from the $x = 0$ end, since the reaction is complete.

The reactant conversion at the $x = L$ end is shown as a function of time in Figure 4. For each pellet length, as discussed above, the conversion increases sharply when the reaction front reaches the end. It may be noted that 99% conversion is achieved in the $L = 3$ pellet at value of $\tau = 4.71$, which is less than one-third of the value of $\tau = 17.34$ for the $L = 9$ pellet. This can be explained by considering that when the conversion front approaches the $x = L$ end, it undergoes an acceleration due to the increase of temperature caused by the adiabatic condition at $x = L$, as illustrated in Figure 5. Specifically, as the front proceeds along the pellet, heat is continuously transferred to the material ahead of the front by conduction. Once the front approaches the $x = L$ end, due to the adiabatic condition (Eq. 15), this mechanism does not operate any longer and then the temperature increases sharply, as shown in Figure 2a.

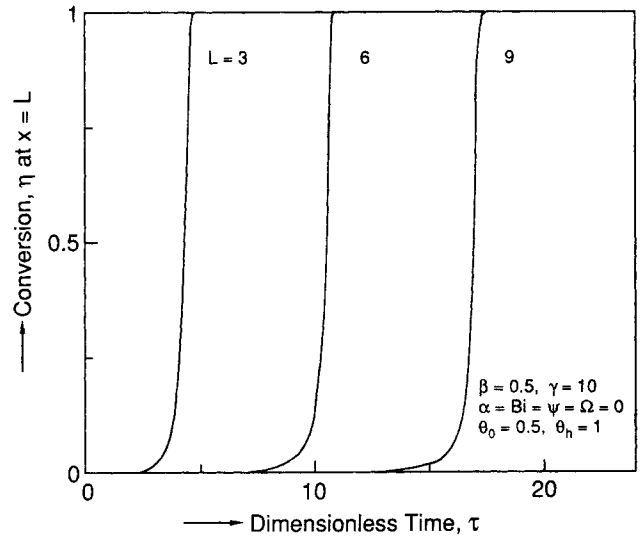

Figure 4. Conversion at the end of the pellet as a function of time.

When considering the same overall amount of material in three pellets of $L = 3$ or one of $L = 9$, the above acceleration phenomenon at the $x = L$ end occurs three times more in the first than in the second case. This explains why the time for completing the reaction in the pellet of $L = 3$ is less than one-third of that required in the case of the pellet with $L = 9$.

It should be noted that the above conclusion holds true as long as the reaction proceeds via the propagation of a conversion front (as long as the energy input at the $x = 0$ end is substantial) whether it is provided by the mechanism of Eq. 13 or that of Eq. 14a. If this is not the case, say for the case of BC of Eq. 14 with $\tau_\phi \simeq 0$, the reaction still proceeds at a rate corresponding to the initial temperature, θ_o. In this case, the process approaches the *sintering regime* and the reaction tends to proceed uniformly throughout the pellet *without* the formation of any propagating

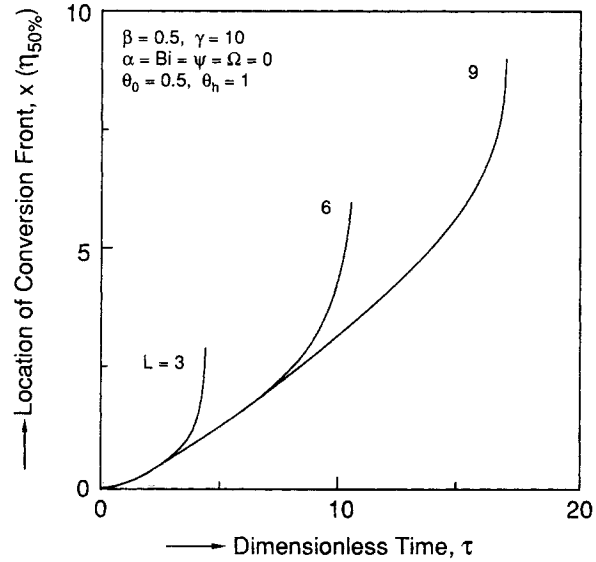

Figure 5. Location of 50% conversion front as a function of time, boundary condition of Eq. 13.

front. In particular, in the case where $\tau_\phi = 0$ in Eq. 14, in addition to $Bi = \Omega = 0$, it can be seen readily from Eqs. 10–12, 14 and 15 that the resulting θ and η are *independent* of the position, x. In this case, the acceleration feature described above does not arise, and the time required for completing the reaction is the *same* for all pellets of any length.

The location of the reaction front, as indicated by the position where the 50% conversion point is located, is shown as a function of time in Figure 5 for three different pellet lengths. For an *infinitely long* system, a constant-pattern behavior exists, in which the reaction front moves with a constant velocity (cf. Novozhilov, 1961; Khaikin and Merzhanov, 1966; Puszynski et al., 1987). Such a behavior would result in a straight line in the plot of conversion front location vs. time. However, such behavior is not observed in Figure 5. The reason is that in a *finite* system, the reaction front movement is influenced by boundary conditions at the ends, while this influence is absent in an infinite system. Thus we can make the important conclusion that *owing to end effects, a constant-pattern behavior cannot exist for a finite system.*

It may, however, be noted from Figure 5 that the two longer pellets have periods in which they exhibit *almost* constant-pattern behavior. This period is longer for the longer pellet, and one can envision from Figure 5 how the constant-pattern behavior would in fact arise for the infinitely long system.

The velocity of the constant-pattern behavior in an infinite system is typically defined as the wave propagation velocity. Accordingly, it is difficult to define a wave propagation velocity for the finite system in the same manner as for the infinite system. A convenient alternative would be to define it as the *mean* velocity of wave propagation, such as Length of pellet/time required for complete (or 99% complete) conversion.

The case of Figure 5 involved the BC given by Eq. 13 at the $x = 0$ end: to ignite the sample, the $x = 0$ end is suddenly elevated to and maintained at temperature θ_h. In Figure 6, corresponding results for the BC given by Eq. 14 are shown, in other words, for the case where ignition is caused by a constant heat flux, ϕ for a relatively short period of time, τ_ϕ. The same

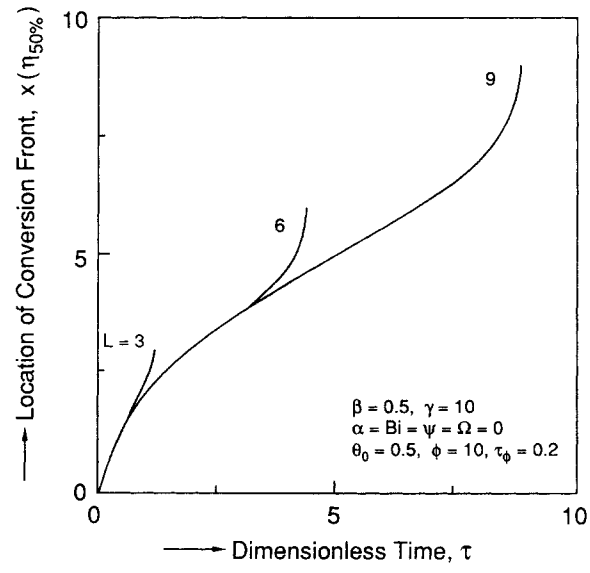

Figure 6. Location of 50% conversion front as a function of time, boundary condition of Eq. 14.

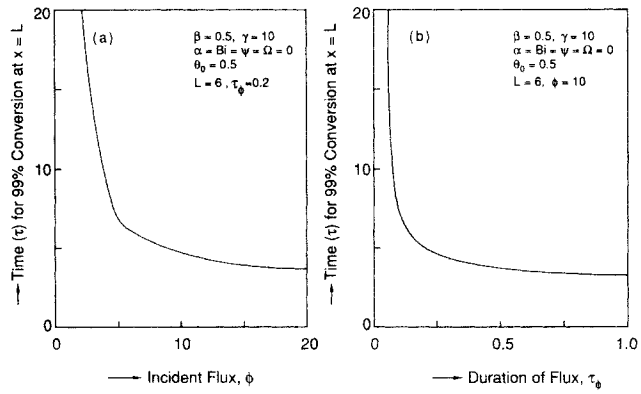

Figure 7. Time required to reach 99% conversion at the $x = L$ end, as a function of: a. supplied heat flux; b. duration of flux.

features, as discussed above in the context of Figure 5, can be seen in Figure 6 as well. The only difference is that the reaction front moves somewhat faster in the case of Figure 6, which as discussed earlier in the context of Figure 3 occurs because higher temperature is attained initially near $x = 0$ for the BC of Eq. 14 for the specific ϕ and τ_ϕ values employed.

The case of the BC given by Eq. 14 is examined further for design purposes in Figure 7. Here, the time required for the reaction to be completed (represented for convenience, by 99% conversion at the $x = L$ end of the pellet) for a fixed value of τ_ϕ is shown as a function of the incident flux, ϕ (Figure 7a) and for a fixed ϕ as a function of the duration of flux, τ_ϕ (Figure 7b). Figure 7a shows that for $\tau_\phi = 0.2$, increasing the incident flux, ϕ, beyond about 10 does not decrease the reaction time significantly. Similarly, from Figure 7b, for $\phi = 10$, increasing the duration of flux, τ_ϕ, greater than about 0.5 leads to only a minor change in the reaction time. Studies of this type can provide useful trade-offs between the magnitude of incident flux, its duration, and processing time.

Nonadiabatic case

For the nonadiabatic case, we first investigated the relative importance of the four types of heat losses: by convection and radiation, and from the surface and the ends. For this, as noted earlier, the range of values of the various dimensionless heat loss parameters (α, Ψ, Bi and Ω) as shown in Table 1 was computed under typical SHS conditions. The results shown in Figure 8, where the influence of α and Bi is assessed one at a time, imply that *convective heat losses do not play a major role in SHS.*

The importance of the radiative heat loss from the surface is assessed in Figure 9. In this figure, the time required for 99% conversion at the $x = L$ end of the pellet is shown as a function of the initial temperature, θ_o for various values of Ψ and all other heat loss parameters (α, Bi and Ω) set equal to zero. It may be seen that for each value of Ψ, the required reaction time increases sharply for decreasing values of θ_o. Furthermore, *for each value of Ψ, there is a critical value of the initial temperature, θ_o below which the reaction front will not self-propagate.* In such cases, the heat generated by reaction is not high enough to overcome the heat losses by radiation to the surroundings and by conduction in the axial direction to self-propagate the reaction front. The results shown in Figure 9

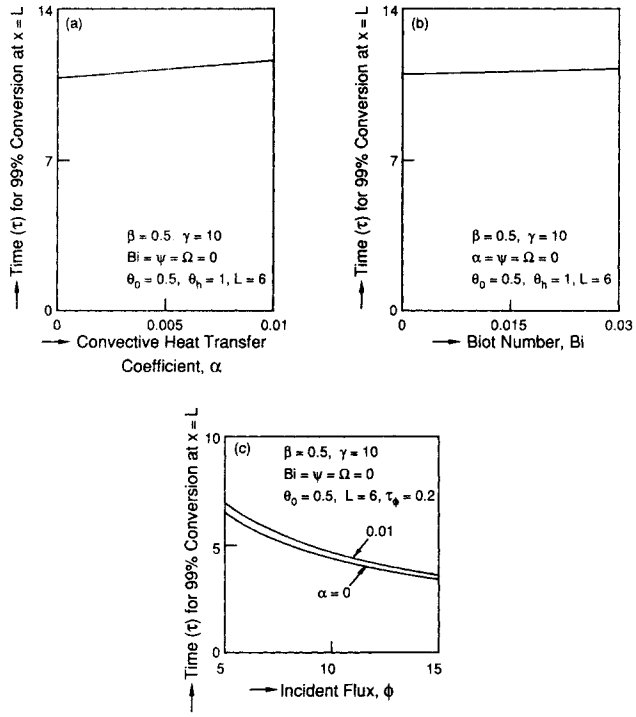

Figure 8. Influence of convective heat losses on the time required to reach 99% conversion at the $x = L$ end.

also indicate that *radiative heat losses from the surface significantly influence the SHS process.*

The importance of radiative heat loss from the ends is also investigated in Figure 9, where two curves at the same value of $\Psi = 0.5$ but with two different values of Ω (0 and 0.3) are shown. It is clear that the presence of a finite Ω further increases the

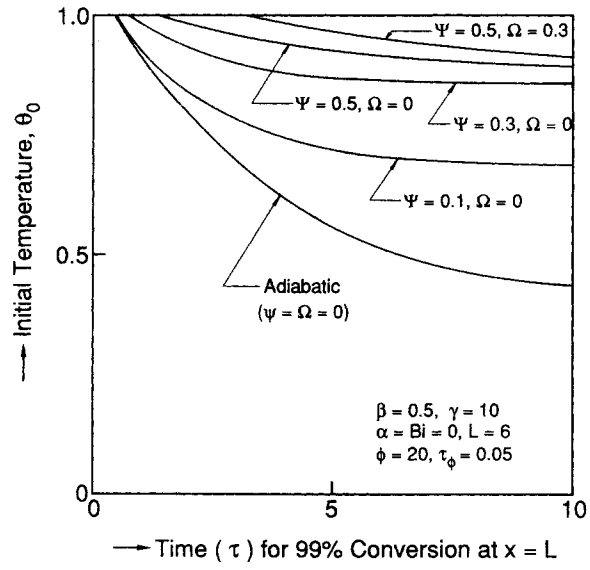

Figure 9. Time required for 99% conversion at the $x = L$ end as a function of the initial temperature, θ_o for radiative cooling parameters from the surface Ψ and from the ends Ω.

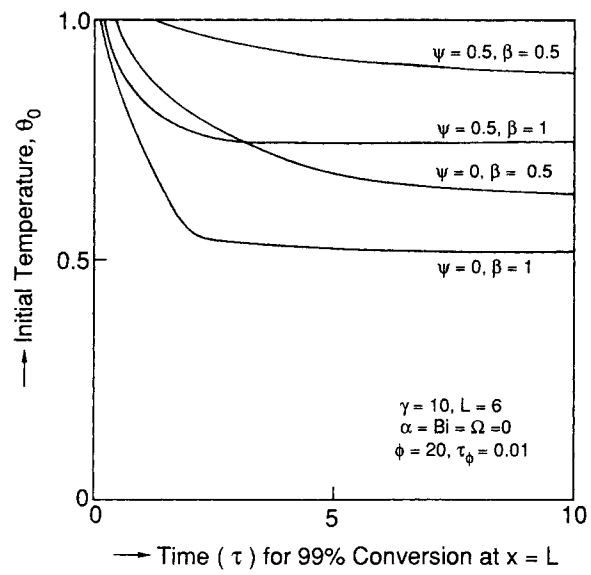

Figure 10. Influence of the heat of reaction parameter β on process performance.

critical value of θ_o. From these results, we can conclude that for the range of parameter values encountered in SHS, the influence of radiative heat loss from the ends (Ω) is important, but it is not as strong as that from the surface (Ψ).

The influence of the heat of reaction parameter, β on process performance is examined in Figure 10. It is apparent that for higher β values, a wider range of initial temperatures, θ_o can be utilized.

For the nonadiabatic case, an example of the reaction front movement is shown in Figure 11. As in the adiabatic case (cf. Figures 5 and 6), it may again be observed that constant-pattern behavior does not exist for finite pellets. Similarly, the $L = 3$ pellet requires a processing time ($\tau = 0.874$) which is less than one-third of the value ($\tau = 3.27$) required for the $L = 9$ pellet.

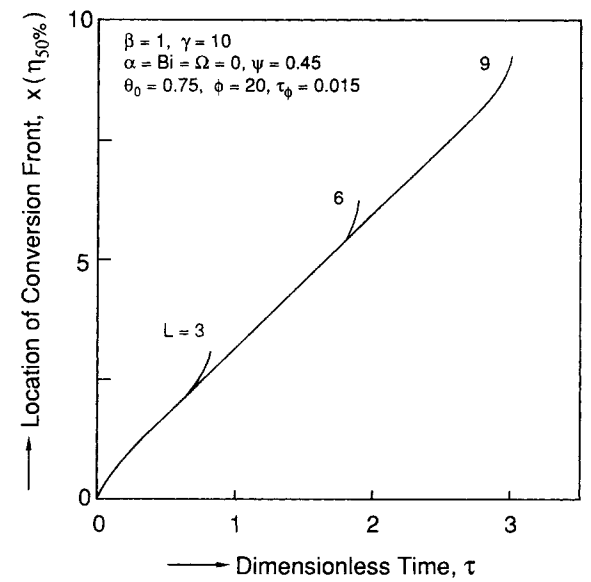

Figure 11. Location of 50% conversion front as a function of time: nonadiabatic case.

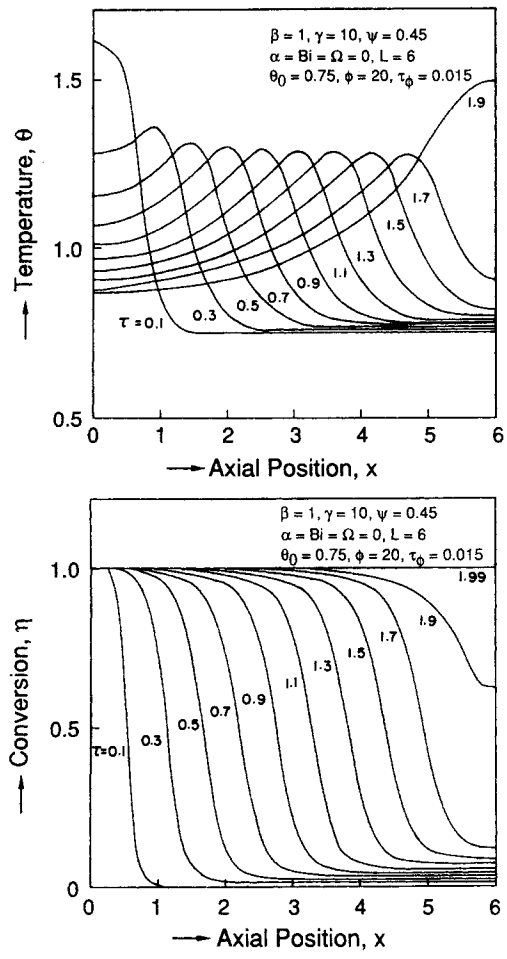

Figure 12. Time-space temperature and conversion profiles for a nonadiabatic case, boundary condition of Eq. 14.

The detailed temperature and conversion profiles for a specific example are shown in Figure 12. For otherwise identical conditions, as compared with the adiabatic case, the velocity of temperature and conversion waves is smaller in the nonadiabatic case. This is because of lower temperature values reached in the pellet due to heat losses, which in particular decrease the heating effect at the $x = L$ end of the pellet (which remains adiabatic in these calculations). The result of this is a smaller acceleration of the reaction front toward the end of the process in the nonadiabatic case, as compared with the adiabatic one, as may be seen by comparing Figures 6 and 11. Note that values for both β and θ_o are higher for the calculations reported in Figure 12 than the corresponding values in Figure 3. The reason for this is apparent from Figure 10. In the nonadiabatic case ($\Psi = 0.5$), even for a higher value of $\beta = 1$, θ_o must be greater than 0.75 in order for the reaction to self-propagate; in the adiabatic case ($\Psi = 0$), the reaction can self-propagate at substantially lower β and θ_o values.

Notation

Bi = Biot number
C_s = reactant concentration
C_p = heat capacity
d = pellet diameter
E = activation energy
F = view factor
k_o = frequency factor
l = pellet length
L = dimensionless pellet length
N = number of interior finite-difference points
r = reaction rate
R = universal gas constant
q = heat flux
t = time
T = temperature
U = Newtonian heat transfer coefficient
x = dimensionless distance
z = distance

Greek letters

α = dimensionless Newtonian heat transfer coefficient
β = dimensionless heat of reaction parameter
γ = dimensionless activation energy
η = conversion
θ = dimensionless temperature
λ = thermal conductivity
ρ = pellet density
σ = Stefan-Boltzmann constant
τ = dimensionless time
ϕ = dimensionless flux
Ψ = dimensionless radiative heat transfer coefficient from the surface
Ω = dimensionless radiative heat transfer coefficient from the end of the pellet

Subscripts

h = value at $x = 0$
o = initial or ambient value

Superscripts

* = reference value

Literature Cited

Bird, R. B., W. E. Stewart, and E. N. Lightfoot, *Transport Phenomena,* Wiley, New York (1960).

Borovinskaya, I. P., A. G. Merzhanov, N. P. Novikov, and A. K. Filonenko, "Gasless Combustion of Mixtures of Powered Transition Metals with Boron," *Combustion, Explosions and Shock Waves,* **10,** 2 (1974).

Gear, C. W., *Numerical Initial Value Problems in Ordinary Differential Equations,* Prentice-Hall, Englewood Cliffs, NJ (1971).

Khaikin, B. I., and A. G. Merzhanov, "Theory of Thermal Propagation of a Chemical Reaction Front," *Combustion, Explosions and Shock Waves,* **2,** 22 (1966).

Kumar, S., J. A. Puszynski, and V. Hlavacek, "Combustion Characteristics of Solid-Solid Systems. Experiment and Modeling," *Int. Symp. on Combustion and Plasma Synthesis of High-Temperature Materials,* San Francisco (Oct. 23–26, 1988).

Merzhanov, A. G., and B. I. Khaikin, "Theory of Combustion Waves in Homogeneous Media," *Prog. Energy Combust. Sci.,* **14,** 1 (1988).

Merzhanov, A. G., and I. P. Borovinskaya, "Self-Propagated High Temperature Synthesis of Refractory Inorganic Compounds," *Dokl. Akad. Nauk SSSR,* **204,** 429 (1972).

Munir, Z. A., "Synthesis of High Temperature Materials by Self-Propagating Combustion Methods," *Ceram. Bull.,* **67,** 342 (1988).

Novozhilov, B. V., "The Rate of Propagation of the Front of an Exothermic Reaction in a Condensed Phase," *Dokl. Akad. Nauk SSSR,* **141,** 151 (1961).

Puszynski, J., J. Degreve, and V. Hlavacek, "Modeling of Exothermic Solid-Solid Noncatalytic Reactions," *Ind. Eng. Chem. Res.,* **26,** 1424 (1987).

Manuscript received Aug. 18, 1989, and revision received May 8, 1990.